Line Tension and Bending Energy: Understanding their effects on phase separation and the formation of modulated phases

Honors Thesis
Presented to the College of Arts and Sciences
Cornell University
in Partial Fulfillment of the Requirements for the Biology Honors Program

by
Sanjula Wickramasinghe
May 2015

Supervisor: Dr. Gerald Feigenson

Abbreviations:

DSPC, 1,2-Distearoyl-sn-glycero-3- phosphocholine; DOPC, 1,2-Dioleoyl-sn-glycero-3-phosphocholine; POPC, 1- Palmitoyl-2-oleoyl-sn-glycero-3-phosphocholine; bSM, brain sphingomyelin; eSM, egg sphingomyelin; pSM, palmitoyl sphingomyelin; POPG, 1-palmitoyl-2-oleoyl-*sn*-glycero-3-phospho-(1'-*rac*-glycerol); C12:0 DiI: 1,1′-didodecyl-3,3,3′,3′-tetramethylindocarbocyanine perchlorate, WALP-23, Ac-GGGAF^{4}F^{5}(LA)$_{6}$LW^{19}LAGA-Amide

ABSTRACT

A chemically simple four-component model of animal cell plasma membranes can mimic some important properties of the far more complex biological mixture. In the compositional region of the model mixture where co-existing liquid-ordered (L_o) and liquid-disordered (L_d) phases coexist, three interesting behaviors were studied: (1) the first appearance of macroscopic phase domains; (2) the line tension between the coexisting domains; and (3) the bending energy of the coexisting domains. A minimal line tension ~ 0.3 pN is required for macroscopic phase domains to form. A range of line tensions just above this minimal value where phase patterns are observed, so-called "modulated phases", which seem to result from line tension competing with other interactions. The bending energy of the L_o phase exceeds that of the coexisting L_d phase, but the addition of a transmembrane α-helical peptide increases the bending energy of the Ld phase but does not significantly affect the liquid ordered phase. Combining these studies sheds some light on the way these energies interact with each other to result in phase separation and modulated phases.

INTRODUCTION

Biological membranes are complex and fascinating but much is unknown about the way they function because of the difficulty associated with studying them. It is difficult to even measure the composition of biological membranes as eukaryotic cells contain membrane bound organelles that also contribute lipids to compositional analysis of the cells. Major components of the outer leaflet of the plasma membrane are sphingomyelins (SM), phosphocholines (PC) and cholesterol (Chol). In contrast, the inner leaflet is mostly comprised of phosphatidylethanolamines (PE), phosphotidylserines (PS) and cholesterol (Feigenson 2007). Including all the acyl chain variations, there are actually hundreds of

different lipid components. Therefore, simplified models of the lipid membranes are often used for biophysical and chemical analysis of the membranes.

An early influential model for the animal cell plasma membrane was the "fluid mosaic" model (Singer & Nicolson 1972). This model was widely accepted by cell biologists, before they understood that lipid membranes are not homogenously mixed over the entire surface but instead can form domains (Samsonov et al. 2001). Simons and van Meer proposed a model of 'lipid rafts' in 1988 after studying epithelial cell polarity. It was noted that the apical membrane contained much less PC and much more glycosphingolipids when compared to the basolateral membrane. It was then proposed that 'lipid rafts' were formed in membranes, with a high cholesterol and SM concentration in the rafts forming liquid-ordered phase (Simons & Toomre 2000; Brown & London 1998; Anderson & Jacobson 2002).

Rafts have several important characteristics that are studied. First, lipid rafts are shown to be thicker than the surrounding domains (Heberle et al. 2013). This was measured by small angle neutron scattering (SANS) experiments at Oak Ridge National Laboratory in Tennessee. Lipid rafts also have organizational functions for proteins in the cell membrane. Proteins in rafts are hypothesized to have functions in signal transduction (Simons & Toomre 2000), transmembrane signaling pathways and receptors (Brown & London 1998), and aid in transport through the membrane.

Since these lipid rafts mimic liquid-ordered phases within a less organized liquid-disordered phase, the lipid membranes I study are modeled in a two phase region of liquid-ordered and liquid-disordered coexistence. The lipid compositions in this region of coexistence can be determined using phase diagrams that are then used to systematically study lipid phase behavior in model membranes. An example of a 3-component phase diagram is shown in **Figure 1**.

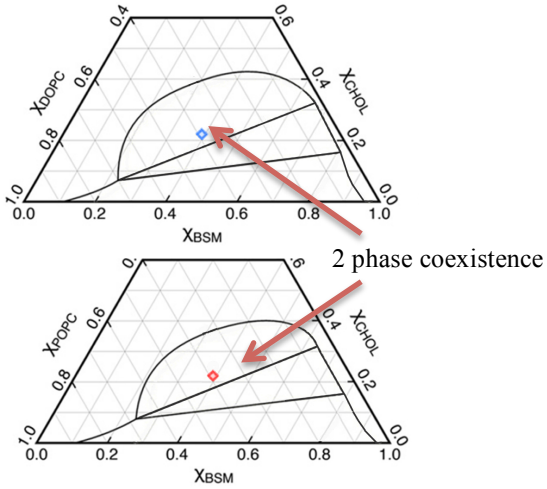

Figure 1 Phase diagram for bSM/DOPC/Chol and bSM/POPC/Chol determined by FRET and DSC. Phase boundaries from Petruzielo et al. (2013).

Accurate boundaries of the phases of the diagram are obtained by using Förster Resonance Energy Transfer (FRET) and Differential Scanning Calorimetry (DSC). The area of L_o and L_d coexistence is well defined and it is especially useful in studying model membranes (Petruzielo et al. 2013; Heberle et al. 2010; Konyakhina et al. 2013). The phase diagram can also be used to determine the regions of gel phase, liquid-ordered and gel phase coexistence and also regions where three phases coexist.

Studying the 2-phase Ld + Lo coexistence has uncovered many interesting facets about model membranes. It is possible to create the 2-phase region by using just 3 components to study the behavior of model membranes. For example, the bSM/POPC/Chol system can be used where bSM (a SM mixture with 18:0 carbon chain lipids being the most abundant) is the high melting lipid and POPC is the low melting temperature lipid. When vesicles are made within the two-phase region, they appear uniform. POPC can be replaced with another low melting temperature lipid, synthetic DOPC. While POPC has one 16-carbon chain and one 18-carbon chain with a double bond, DOPC contains two 18-carbon chains with one double bond in each chain. The change in length and number of double bonds results in macroscopic phase separation (complete separation of the L_o and L_d domains) when

the POPC is replaced with DOPC (**Figure 2C**). The formation of macroscopic domains indicates that there is a possibility of nanodomains existing in the uniform region, but they must be under 200nm in size which is the maximum resolution of an optical microscope (Petruzielo et al. 2013).

It is possible to use four-component model membranes to further study this phase domain size behavior. Other high melting temperature lipids such as pSM and eSM can be used in the place of bSM. pSM contains 16:0 carbon chains while eSM contains a mixture of SMs with the 16:0 carbon chain being the most abundant. A mixture of low melting temperature lipids is also used. For example, I can start with a system that is bSM/POPC/Chol and replace the POPC with DOPC using the replacement ratio of ρ defined as

$$\rho = \frac{DOPC}{DOPC + POPC} \qquad (1)$$

As the fraction of DOPC is steadily increased, the morphology of the vesicles start to change as seen in **Figure 2**. At a certain ρ value, the morphology changes to 'modulated phases', which present as stripes or a honeycomb pattern of L_d and L_o domains on GUVs (Giant Unilamelar Vesicles) (Goh et al. 2013).

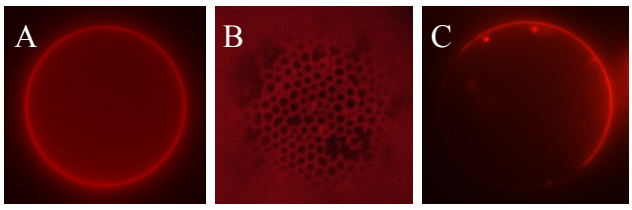

Figure 2 GUVs imaged using fluorescence microscopy with C12:0 DiI showing **A** uniform, **B** modulated and **C** macroscopic phase separation of a bSM/DOPC+POPC/Chol system. The dye partitions favorably into the L_d domain, which fluoresces red.

The formation of these modulated phases is thought to be a result of competing interactions between line tension and bending rigidity. Through simulation studies it was shown that different combinations of relative and discrete values for line tension and bending

energy yielded different patterns such as striped, modulated or macroscopic phase separation (Amazon et al. 2013). The simulation studies showed that line tension has a dominant effect on the morphology of the vesicles, and when coupled with certain bending energy values, modulated phases formed. However, slight changes to these values can perturb this morphology and either melted (uniform phase) or macroscopic phase separations can form. To understand this interaction it is important to first understand what is meant by line tension and bending energy.

Line tension at the boundaries between coexisting fluid domains is defined as being the energy per unit length of a boundary. This follows the definition of surface tension but on a two-dimensional plane. In terms of lipid membranes it helps to explain how a circular fluctuating raft can resume its shape after an external perturbation has been applied to it (Kuzmin et al. 2005). All the factors that go into the function that presents as line tension are still not fully understood. The main factors are thought to be height mismatch between the L_o and L_d domains (Heberle et al. 2013), spontaneous curvature of the domains as a result of the splay and tilt of the lipid molecules (Kuzmin et al. 2005) and the dipole-dipole repulsion of lipids within the domains (Konyakhina et al. 2011). Line tension has been proposed to play a part in the control of membrane deformation, budding and fission of the membrane (Baumgart et al. 2007). If one large domain were to form, the system would have a lower total line energy value. Opposing factors to forming one large domain are the decrease in energy of bending on a curved surface, and a decrease in dipole-dipole repulsion in small versus large domains (Amazon & Feigenson 2014). This idea is used to model the line tension studies in the hopes to understand the formation of modulated phases.

Theoretical values of line tension have been calculated to be on the order of 10^{-11}N. This value has been confirmed experimentally using several methods. For the system of SM/DOPC/Chol, a line tension value of ~1pN has been obtained using micropipette

aspiration (Baumgart et al. 2003). This method allows line tension measurements up to 5pN but values under 0.5pN are thought to be inaccurate (Esposito et al. 2007). Another method, Flicker Spectroscopy, in which the fluctuations of the domains are studied, also yielded line tension values on the order of 1pN (Esposito et al. 2007). With further measurement and study of line tension it was proposed that line tension values greater than 4pN would result in complete phase separation (Frolov et al. 2006).

Line tension is measured using Flicker Spectroscopy as described by Esposito et al., (2007). Line tension was measured experimentally by using fluctuation spectroscopy and capillary wave theory. In brief, the mode amplitudes (u_n) of the Fourier transform of a fluctuating domain's perimeter are related to line tension by the equation:

$$< u_n >^2 = \frac{2K_B T}{\sigma \pi R_o (n^2 - 1)} \qquad (2)$$

where k_B is the Boltzmann constant, T is the temperature, σ is line tension, R_o is the radius of the fluctuating domain and n is the mode (frequency) number.

The other main factor in the formation of modulated phases is the difference in bending energy of the domains in the membrane. Some of the first studies of bending rigidity used the budding of L_o and L_d phase-separated vesicles as seen in **Figure 3**.

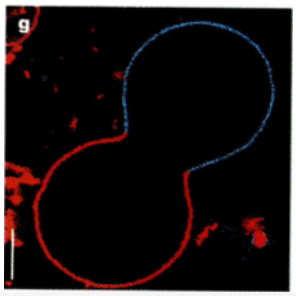

Figure 3. GUV used to measure bending energy that exhibit liquid phase coexistence with budding off of one phase. The L_o domain is stained with perylene (blue) and the L_d domain is stained with rho-DPPE (red). Image from Baumgart et al. (2003).

Analysis of the L_d domains of the neck region of the budding vesicles showed that L_d domains bend towards the L_o domains, suggesting that L_o domains are stiffer. This is supported by the finding that L_o phases exhibit smaller amplitudes of thermally excited

fluctuations of the single phases (Baumgart et al. 2003). The bending energy is measured by imaging the fluctuations of the distinct phases, usually on a budding vesicle as shown in **Figure 3** (Baumgart et al. 2005; Semrau et al. 2008). The difference in bending energies of the phases, L_o being stiffer than L_d, determines which phase is the continuous phase when modulated phases are observed. For all the GUVs in the modulated phase region, the L_d phase is continuous, because the L_o phase is stiffer and therefore more difficult to bend over the surface of the GUV.

Bending energy is measured by making L_d and L_o single phase GUVs. Bending energy was experimentally determined by using fluctuation analysis and capillary wave theory. Similar to line tension, the bending energy k was related to the dimensionless mode amplitude (U_{lm}) by

$$< |U_{lm}|^2 = \frac{K_b T}{k(l+2)(l-1)\left[l(l+1) + \frac{\sigma_{eff} R^2}{k}\right]} \qquad (3)$$

Here K_bT is the thermal energy and σ_{eff} is the effective tension of the vesicles and R is the radius of the GUV.

Proteins often are required to mediate changes in membrane curvature, for example in highly curved raft structures such as virus budding sites and brush-border epithelial cells (Baumgart et al. 2005). Addition of proteins or peptides allows a systematic study of bending energy in order to lend an understanding to the formation of modulated phases. To imitate the effects of peptides on the model membranes, I added WALP-23, a transmembrane helical peptide in varying concentrations to our samples for the model membrane.

To understand the physical properties of phase separation and the formation of modulated phases in model cell membranes the study was broken into three parts: measuring ρ windows, line tension, and bending energy.

MATERIALS AND METHODS

The systems used in these studies mimic the outer membrane of the biological membrane and so consist of PCs, SMs and cholesterol. The PCs and SMs were purchased from Avanti Polar Lipids (Albaster, AL) and the purity of the lipids was tested by thin layer chromatography, and the concentration of the lipid stocks is measured by an inorganic phosphate assay (Kingsley, P. B., Feigenson 1979). POPC and DOPC are the low melting lipids. pSM, eSM and bSM are the high melting temperature lipids with a transition temperature of 45°C. It is important to note that eSM and bSM are both mixtures of several different sphingomyelins. Cholesterol was obtained from Nu Chek Prep (Elysian, MN) and it was prepared at a defined concentration using standard gravitation procedures. C12:0 DiI (a lipophilic fluorescent dye that preferentially partitions into the L_d phase) was purchased from Invitrogen (Carlsbad, CA) and its concentration was verified by using absorption spectroscopy.

The ρ window, line tension and bending energy measurements were measured by making GUVs by one of two methods. For ρ window measurements, GUVs were made by electroformation as described by Angelova et al. (1992) with several modifications. For this method, the lipids being used for the GUVs were mixed together with the dye in test tubes at the appropriate concentrations in chloroform. This solution was spread on ITO (Indium Tin Oxide) coated slides that are able to conduct a current. The lipid films that formed after evaporation in a vacuum were swelled at 45°C (the transition temperature for the high melting temperature lipids) in 100mM sucrose under the influence of an AC field for 2 hours to form the GUVs. The slides were cooled to room temperature (21°C) over 10 hours and the vesicles were harvested into a glucose solution of around 100mM in glass test tubes. The samples were allowed to sit for 40 minutes to an hour so that the GUVs containing sucrose

solution could settle through the less dense glucose solution. This resulted in a higher yield of the GUVs and also removed any junk from the GUVs.

Images for ρ windows were taken by finding GUVs using phase contrast, and then taking z-stack, a series of images along the z-axis of a region of interest, with fluorescence. C12:0 DiI had been added to the samples at a ratio 1:7500 before spreading the chloroform solution on the ITO slides. The excitation and emission maxima are 549/565 nm, so the sample fluoresces red. No more than 8 z-stacks of images were taken for each slide to avoid the possibility of light-induced artifacts. The number of GUVs counted was between 30 and 60 for each ρ value for all the systems.

For line tension measurements, the GUVs were formed in the same manner using ITO slides and the applied AC field but were cooled in different ways to form domains of a suitable size (see below). For lower ρ values, the GUVs were cooled to room temperature over 3.5 hours and then were harvested into 100mM glucose solution. For higher ρ values, the GUVs were cooled from 45°C to room temperature over 10 hours and harvested into the glucose solutions. These solutions were then warmed up to 50°C and 4µl were added to a slide at room temperature so the solutions cooled over a few seconds. For higher ρ values for the bSM/DOPC+POPC/Chol system the harvested solution was warmed up to 50°C and placed on a slide that had been cooled to 0°C by placing the slide on ice (the side that would not touch the sample was in contact with the ice). The sample was allowed to return to room temperature before imaging.

A Nikon Eclipse TI microscope and a Zyla 5.5 sCOMOS camera from Andor Technologies were used for the line tension measurements. For the measurements, it was important to look for circular domains that were situated at the top of a GUV (the surface of the GUV that was not resting on the coverslip). The domain had to be at least 5 µm in diameter but less than $1/5^{th}$ of the diameter of the entire vesicle. This was important to

minimize bending of the domain over the surface of the vesicle. The short exposure time required to capture the fluctuations of the domains required a high contrast between the L_d and L_o domain. Therefore, C12:0 DiI was added at a ratio of 1:500 to provide a high contrast between the L_o and L_d phases, almost 10 times greater than the normal dye concentration used when identifying ρ windows. A suitable domain was found by looking at the samples under low light intensity. The low light intensity is required to prevent the formation of light induced artifacts (see discussion). Once a suitable domain was found, a time series was taken for 500 frames with a 10ms exposure time at 20ms intervals for a total of 15 seconds.

The fluctuations of the domains were analyzed using Matlab2014b's canny edge detection using the largest domain in the field of view. For the domain in each frame to be considered valid for the analysis of the line tension, the domain had to have closed boundary that was approximately circular. The domain was also considered invalid if the area of the domain varied by more than 3% during the time series. The Fourier transform for each domain was used to calculate σ using **Equation 2**. The line tension for each domain was the calculated over modes n=2-5. This line tension value for each domain was only accepted if there were more than ~250 valid frames and the line tension for each mode was relatively constant.

For bending energy measurements, GUVs were made by using gentle hydration, first introduced by Reeves & Dowben (1969) and modified by Akashi et al. (1996). Similar to electroformation, lipid films are spread on the inside of glass tube and hydrated at 45°C to make sure the lipids were all melted and well mixed before GUVs were formed. 2mol% of a charged lipid, POPG, is added to the lipid mixtures to facilitate the separation of the lipid layers to form GUVs during the hydration steps (Nelson et al. 2010). This addition of the charged lipid does not affect the morphology of the GUVs observed. Sucrose solution was added to the test tubes to swell the lipid layers and form GUVs. The GUVs were harvested

into glucose solution. Gentle hydration has a lower yield than electroformation but electroformation yields a wide range of vesicle tensions. To further ensure that vesicle tensions would not play a part in the bending energy measurements, the sucrose solution is made to be ~5mM lower in osmolality than the glucose solution. The osmolality of the glucose and sucrose solutions were measured using a Precision Systems Osmometer.

The bending energy of the GUVs was ascertained by measuring the fluctuations at the equator of a GUV of a single phase, either L_o or $L_{d,}$ imaged under phase contrast. The compositions of the GUVs were chosen as those in coexistence using the accurate phase diagrams for bSM/DOPC/Chol and bSM/POPC/Chol (Petruzielo et al. 2013). Approximately 1500 frames are taken for each GUV at 1ms exposure times with 20ms wait time. The exposure time had to be 1ms or less so that high wavenumber modes of the fluctuations would not be averaged out, but had to be greater than 10μs to fall within the limits of the optical resolution of the microscope and camera (Gracià et al. 2010). The vesicles had to be unilamellar, which was determined by doing a line scan of fluorescence intensity (C12:0 DiI was added to the samples). If the GUV was unilamellar, the fluorescence intensity doubled. If the vesicles were grown in glucose solution and harvested into a glucose solution, the glucose symmetry across the vesicles would prevent any effect of the gravity on the vesicles (Gracià et al. 2010). However, since GUVs were made using gentle hydration and the yield of gentle hydration is low, the GUVs could not be grown in and harvested into glucose solutions. The density difference between the glucose and sucrose was necessary to purify the GUVs and collect enough GUVs at the bottom of the test tube to be collected and imaged. To compensate for this and minimize effects of gravity on the bending energy measurements, only GUVs that had a radius between 10 and 22μm were imaged.

The fluctuations of the equator of the GUV were analyzed in the same manner as for line tension using Matlab2014b's canny edge detection. For a GUV to be valid, the equator

had to be approximately circular and the radius of the GUV could not vary by more than 25% compared to the previous valid frame. The center of the domain had to be centrally located in the region of interest during the entire time series to ensure that the GUVs being analyzed were not drifting in solution on the slide.

RESULTS

Identifying ρ window

The first part of the project was to study the ρ window for several different four-component systems. The ρ window is defined as the range of ρ values for which more than 50% of the GUVs show modulated phases. The compositions were made at a 0.39/0.39/0.22 ratio of SM/DOPC+POPC/Chol. This composition was chosen as it is in the two-phase coexistence region and is halfway between the L_o and L_d single-phase region. Therefore the area fractions of the L_o and L_d domains would be approximately equal. All three systems show a transition from uniform to modulated to macroscopic phase separation as seen in **Figure 2**.

As seen in **Figure 4,** the bSM/DOPC+POPC/Chol system has the highest ρ window with a center around ρ = 0.55 and egg-SM has a lower ρ window with a center at ρ = 0.10. PSM presented slightly differently as modulated and macroscopic phases were observed for the pSM/POPC/Chol mixture with only a few uniform vesicles detected and was completely macroscopically phase separated by ρ = 0.15. As this was unusual behavior, to ensure that the phase separation that was occurring was not an artifact of the AC field that was applied to the lipid films, samples were made using gentle hydration. Similar ratios of GUVs of each morphology were observed showing that the formation of modulated phases for the pSM/POPC/Chol system was a property of the lipid composition itself and not an artifact of the preparation of GUVs.

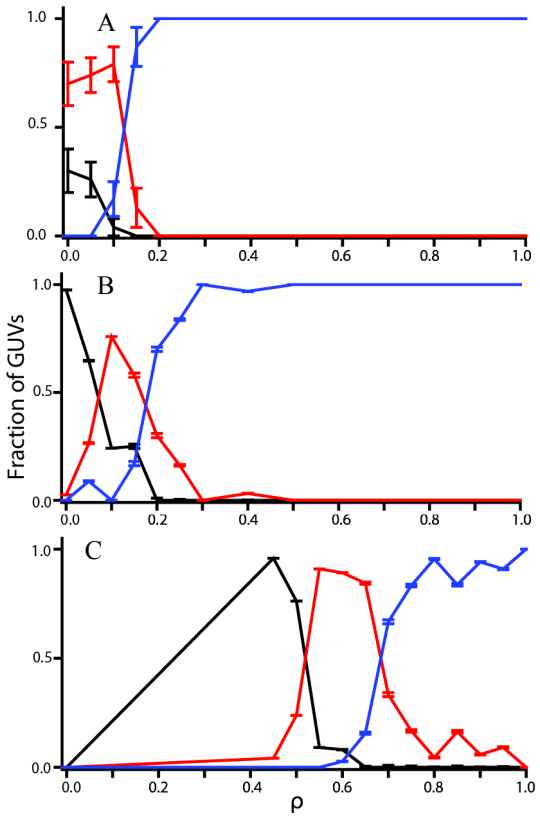

Figure 4 Rho windows for **A** pSM, **B** eSM and **C** bSM with DOPC+POPC and Chol. The fraction of GUVs that show uniform (black), modulated (red) and macroscopic (blue) phase separation are shown. The GUVs were at the composition of .39/.39/.22 for SM/DOPC+POPC/Chol. Error bars: mean ± SE

To test the effect of peptides on the ρ window in the model systems, WALP-23, was added to the bSM/DOPC+POPC/Chol system at 2mol% and 4mol% and the ρ window was measured as before. The resulting figure shows a downward shift of 0.20 in ρ for each consecutive addition of 2mol% of WALP-23 as seen in **Figure 5**.

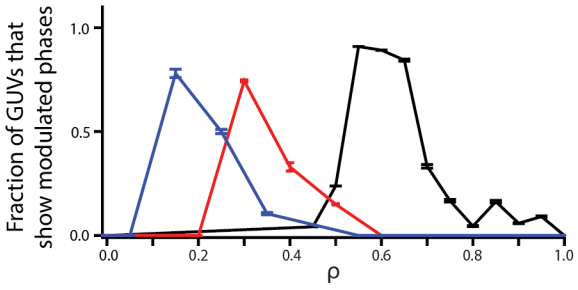

Figure 5 ρ windows for bSM/DOPC+POPC/Chol with the no WALP (black), 2mol% of WALP (red) and 4mol% of WALP (blue). The GUVs were at the composition .39/.39/.22 for SM/DOPC+POPC/Chol. Error bars: mean ± SE

Measuring Line Tension

Line tension was measured for three systems as a function of increasing ρ. For all three systems, where the ρ windows start, or modulated phases are first seen, the line tension values are between 0.3 and 0.5pN. Where the ρ window ends the line tension values are between 0.7 and 1pN and there is an upward trend of line tension with increasing ρ as seen in **Figure 6**. It was possible to measure line tension values for the entire ρ trajectory of pSM/DOPC+POPC/Chol because phase separation was visible at ρ = 0 for this system.

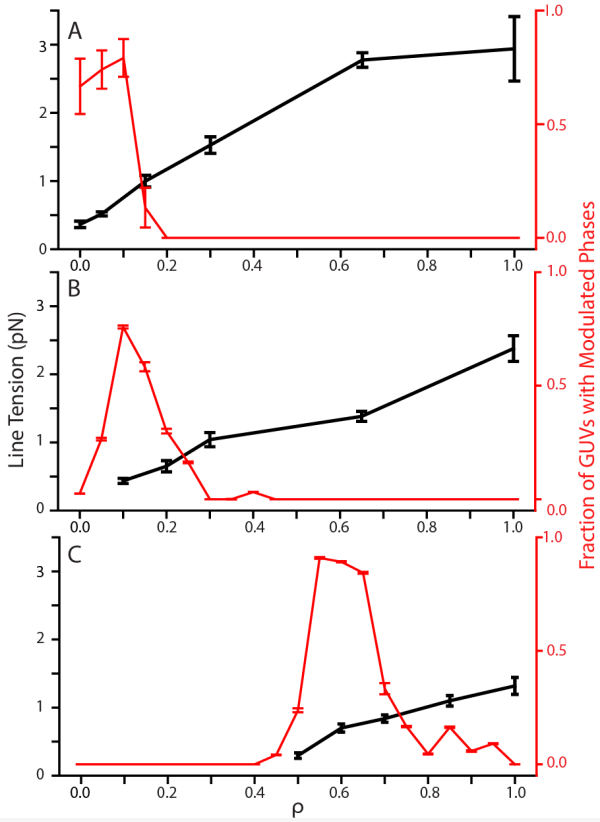

Figure 6 Line tension values (black) and modulated phase GUV fractions (red) for **A** pSM **B** eSM **C** bSM with DOPC, POPC and Chol. . The systems all contain measurements taken after forming the domains through fast cooling (a few seconds) and slow cooling (3.5 hours). Error bars: mean ± SE

The relationship between the amplitude of fluctuations and the value of line tension is visible when imaging the domains. Domains with small amplitudes of fluctuation have higher line tension values and domains with larger amplitudes of fluctuations have lower line

tension values as seen in **Figure 7.** The area of the domains remained the same throughout the time series.

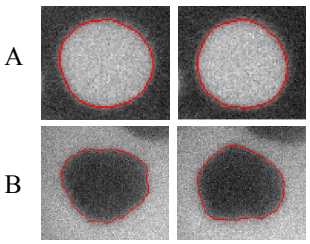

Figure 7 Domains for bSM/DOPC+POPC/Chol showing fluctuations. **A** is at ρ=1.0 with line tension of 1.31±0.12pN. **B** is at ρ=0.5 with line tension of 0.29±0.04pN.

Line tension was measured with the addition of 4mol% of WALP. The values of line tension where the ρ window starts and end remain similar to the values of line tension without WALP as seen in **Figure 8**. A similar upward trend in line tension values was observed. It is important to note that the line tension value at ρ = 1 with the addition of WALP (0.98±0.15pN) was slightly lower than the value at ρ = 1 without WALP (1.31±0.12pN).

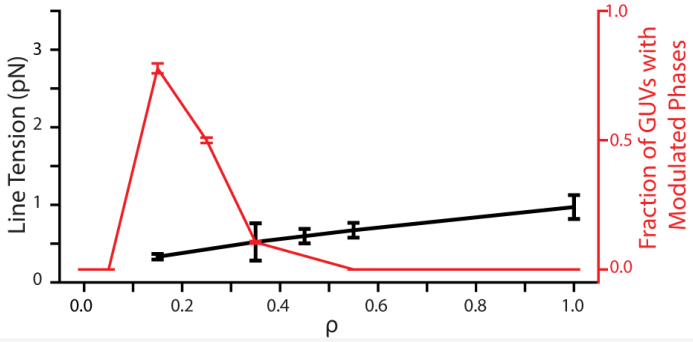

Figure 8 Line tension values (black) and modulated phase GUV fractions for bSM/DOPC+POPC/Chol with 4mol% of WALP. Error bars: mean ± SE

Since the GUVs had to be cooled using different methods to obtain the required domain size to analyze line tension, it was important to check that the values obtained were not affected by the different cooling methods. To ensure that this was not the case, GUVS for pSM/DOPC+POPC/Chol and eSM/DOPC+POPC/Chol were cooled over 3.5 hours and another set of samples were cooled over a few seconds. Only GUVs of certain ρ values would

form the required domains using both methods. The results show that for these ρ values, the line tension values were within the error values of each other as shown in **Figure 9.**

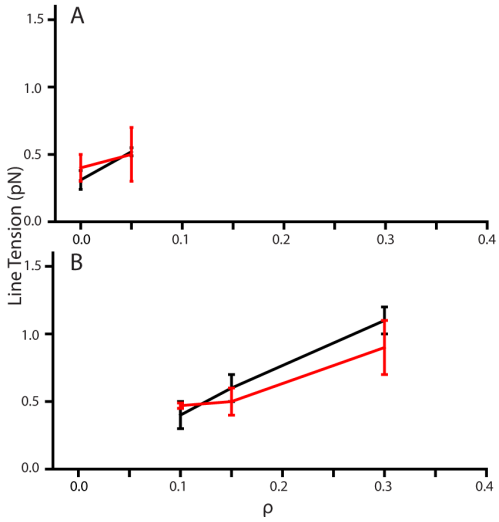

Figure 9 Line tension measurements using fast cooling (black) and slow cooling (red) for **A** pSM and **B** eSM with DOPC, POPC and Chol.

Measuring Bending Energy

Bending energy measurements were taken for single phase L_o and L_d domains for bSM/DOPC/Chol and bSM/POPC/Chol at increasing concentrations of added WALP. For both DOPC and POPC, the bending energy of the L_d phase is lower than that of the L_o phase. The bending energy of the L_d phases increases significantly with the addition of only 1mol% of WALP. With the addition of 4mol% the values are 2.65 and 2.8 times greater in magnitude for the DOPC and POPC containing mixtures respectively. The bending energy of the L_o phases does not change significantly, even at 4mol% of WALP. So after the addition of the peptide, bending energy of the L_d phase is greater than the bending energy of the L_o phase showing that the L_d phase becomes stiffer than the L_o phase. From the data observed, addition of less than 1mol% of WALP to the mixtures would increase the stiffness of the L_d phase compared to the L_o phase.

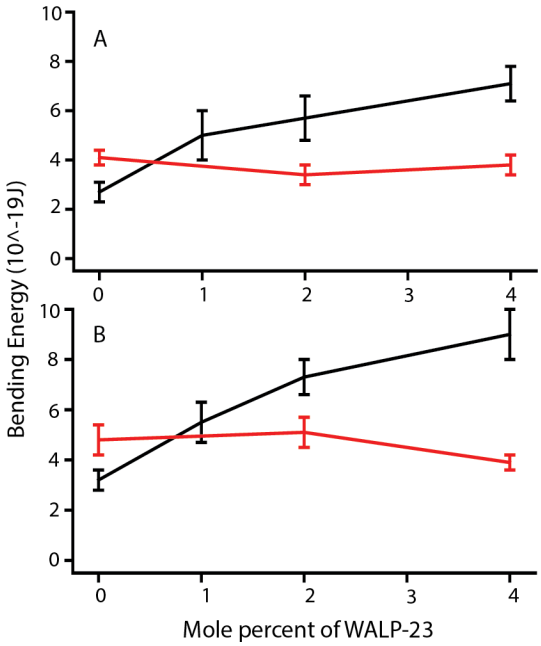

Figure 10 Bending energy values for **A** bSM/DOPC/Chol and **B** bSM/POPC/Chol for L_d phase (black) and L_o phase (red). The compositions of the GUVs were as follows: bSM/DOPC/Chol L_d .21/.72/.07 L_o .65/.01/.34; bSM/POPC/Chol L_d .24/.68/.08 L_o .62/.05/.33

DISCUSSION

Line Tension Overcomes The Free Energy Barrier Of Domain Coalescence

Line tension has been measured before through several different methods (Esposito et al. 2007; Tian et al. 2007; Baumgart et al. 2003; Semrau et al. 2008). However, line tension has not been measured systematically as the phases of the GUVs shift from uniform to modulated to macroscopic. By doing so, I was able to determine the average line tension of the system that would result in the macroscopic phase separation. The theoretical and experimental line tension values measured for GUVs were on the order of 1pN (Semrau et al. 2008) are similar to the results obtained in this study.

As shown by the ρ windows obtained for the three systems, travelling along a ρ trajectory starting at ρ = 0 results in phase separation and the total length of the boundaries decreases. As ρ increases, the boundary is minimized as the GUVs become macroscopically

phase separated and round up into a single phase-separated domain. In this state, the boundary is at its minimum value. With increase in ρ, the line tension increases, so minimizing the total perimeter, hence minimizing the total line energy occurs when the smaller domains coalesce to form two large domains of L_o and L_d.

Line Tension As Nanodomain Proof

It is has been suggested through FRET, ESR (Electron Spin Resonance), and SANS studies that uniform vesicles can actually contain nanodomains on the order of 10nm (Heberle et al. 2010). The stability of these small domains would require very low line tension values and free energy that would prevent the formation of larger domains. The trends of the line tension data observed show that within the modulated phase region as you travel down the ρ trajectory, the line tension continues to decrease, reaching values between 0.3 and 0.5pN (**Figure 7).** This suggests that within the uniform region of the ρ trajectory, the line tension could continue to drop, resulting in very low values of line tension for the nanodomains.

However, it is not possible to measure line tension without visible domains, so in the uniform region of the ρ trajectory, it is not possible to say that the line tension drops to zero as ρ continues to decrease. Since pSM is an unusual case and does not require any DOPC to induce phase separation at ρ = 0 there is a finite value for line tension. Hypothetically, it is likely that the systems containing eSM and bSM would also behave in a similar manner and reach a finite low value of line tension that would result in the formation of nanodomains.

Light-Induced Artifacts In Line Tension Measurement

Measurement of line tension requires illuminating the samples with high intensity light for a total of several seconds on a sample containing relatively high dye concentration. Shining high intensity light on GUVs has been shown to induce artifactual phase separation (Nelson et al. 2010). These artifacts could present as breaking up of domains in to smaller

ones, the fusion of two domains to form a larger one or a change in the amplitudes of the fluctuations of the domains. To minimize the formation of artifacts, including having the fluctuations of the domains affected by the intensity of the light, the intensity of light was kept at 50% of the full possible intensity of the Lumincore LED illumination system of our microscope. The concentration of dye was reduced to 1:500 instead of the 1:250 dye ratio that was first tested. As a precaution a maximum of 8 domains were imaged for each sample slide that was made.

However, since the light intensity and dye concentration for these domains are high, to ensure that the light did not induce any changes in the line tension measurements, the 500 frames in the time series were divided into sets of five and the line tension was plotted as line tension versus time for domains at each ρ value (data not shown). This showed that the fluctuations in the line tension value for the different sets of frames but it did not change by more than 20% and there was no overall trend in the change of the line tension for all the ρ values for each system. When line tension was plotted against ρ, the values and overall trends in line tension also remained the same (data not shown).

L_o Is Stiffer Than L_d

The measured values for the L_d phases were $2.70\pm0.3*10^{-19}$ and $3.20\pm0.4*10^{-19}$ for DOPC and POPC respectively. For L_o phases the values are $4.10\pm0.3*10^{-19}$ and $4.80\pm0.6*10^{-19}$J respectively. These values are on the same order as other measured bending energy values (Semrau et al. 2008). The values also showed that the L_o phase was much stiffer than the L_d phase. This is expected, as the continuous phase in the modulated phase GUVs is the L_d phase. Since this phase is less stiff, it can bend over the surface of the GUV with less of an energy penalty.

Addition Of WALP Stiffens The L_d Phase

WALP-23 is a transmembrane peptide that has a partition coefficient of 10 into the L_d phase in the bSM/DOPC+POPC/Chol system and 1.8 into the L_o phase in the bSM/DOPC+POPC/Chol system. The partition coefficient studies were measured using FRET (unpublished, Thais Enoki). The phase boundaries were measured after the addition of 1 and 2mol% of WALP using FRET and the phase boundaries had not shifted, so the lipid compositions that resulted in the single phases were not affected by this addition (Enoki & Simpson, unpublished).

However, with the addition of 4mol% of WALP to the GUVs, the bending energy of the phases increases almost 3-fold for the L_d phases but does not change for the L_o phases. As WALP partitions preferentially into the L_d phase, the accumulation of WALP stiffens this phase. This suggests that the WALP could have an effect on the order of the lipids in the L_d phase.

Line Tension And Bending Energy As Factors Of Phase Formation

With the line tension data that was acquired it is possible to draw a link between increasing line tension and phase separation for the four-component model membranes as DOPC is added to the system to induce phase separation. It can also be determined that certain values of line tension are required for phase separation to occur in the model membrane.

With the addition of WALP to the bSM/DOPC+POPC/Chol system, there was a shift to lower values for the ρ window. When line tension is measured for this system with the addition of WALP, the values of line tension where the ρ window starts and ends are shown to be similar to the values of line tension without any WALP. The addition of WALP raises the line tension in what was formerly the uniform region of the ρ window. This suggests that the difference in stiffness of the domains would change the amount of the DOPC required to

induce phase separation, i.e. change the ρ window but that the line tension is the more important factor in determining where the modulated phases appear.

FURTHER DIRECTIONS

To be able to fully understand the effect of competing interactions of line tension and bending energy, more systems have to be studied. For line tension, the values should be measured with different high and low melting temperature lipids and mixtures of the lipids to better mimic a biological cell membrane. Since all these measurements were taken at a ratio of .39/.39/.22 of SM/DOPC+POPC/Chol, it would also be beneficial to see if changing the composition of the system within the two phase coexistence region would hold the same results. Specifically, increasing the amount of cholesterol in the system so that the ratio of lipids is closer to the biological ratio found in cell membranes.

To further study the effects of WALP addition to the GUVs different lengths of the peptide, WALP-19 and WALP-23 could be used, to see the effects of the length of the peptide on the bending energy of the different phases.

ACKNOWLEDGEMENTS

Thais Enoki measured the partition coefficient of WALP. Rebecca Simpson and Thais Enoki measured the phase boundaries with the addition of WALP. Denise Greathouse and Roger Koeppe at the University of Arkansas provided the WALP-23 used in these studies.

REFERENCES

Akashi, K. et al., 1996. Preparation of giant liposomes in physiological conditions and their characterization under an optical microscope. *Biophysical journal*, 71(December), pp.3242–3250.

Amazon, J.J. & Feigenson, G.W., 2014. Lattice simulations of phase morphology on lipid bilayers: Renormalization, membrane shape, and electrostatic dipole interactions. *Physical Review E - Statistical, Nonlinear, and Soft Matter Physics*, 89, pp.1–11.

Amazon, J.J., Goh, S.L. & Feigenson, G.W., 2013. Competition between line tension and curvature stabilizes modulated phase patterns on the surface of giant unilamellar vesicles: A simulation study. *Physical Review E - Statistical, Nonlinear, and Soft Matter Physics*, 87, pp.1–10.

Anderson, R.G.W. & Jacobson, K., 2002. A role for lipid shells in targeting proteins to caveolae, rafts, and other lipid domains. *Science (New York, N.Y.)*, 296(June), pp.1821–1825.

Angelova, M., Soleau, S. & Méléard, P., 1992. Preparation of giant vesicles by external AC electric fields. Kinetics and applications. *Trends in Colloid and ...*, 89(899), pp.127–131. Available at: http://link.springer.com/chapter/10.1007/BFb0116295.

Baumgart, T. et al., 2007. Large-scale fluid/fluid phase separation of proteins and lipids in giant plasma membrane vesicles. *Proceedings of the National Academy of Sciences of the United States of America*, 104(9), pp.3165–3170.

Baumgart, T. et al., 2005. Membrane elasticity in giant vesicles with fluid phase coexistence. *Biophysical journal*, 89(August), pp.1067–1080.

Baumgart, T., Hess, S.T. & Webb, W.W., 2003. Imaging coexisting fluid domains in biomembrane models coupling curvature and line tension. *Nature*, 425, pp.821–824.

Brown, D. a & London, E., 1998. Functions of lipid rafts in biological membranes. *Annual review of cell and developmental biology*, 14, pp.111–136.

Esposito, C. et al., 2007. Flicker spectroscopy of thermal lipid bilayer domain boundary fluctuations. *Biophysical journal*, 93(November), pp.3169–3181.

Feigenson, G.W., 2007. Phase boundaries and biological membranes. *Annual review of biophysics and biomolecular structure*, 36(December 2006), pp.63–77.

Frolov, V. a J. et al., 2006. "Entropic traps" in the kinetics of phase separation in multicomponent membranes stabilize nanodomains. *Biophysical journal*, 91(July), pp.189–205.

Goh, S.L., Amazon, J.J. & Feigenson, G.W., 2013. Toward a better raft model: Modulated phases in the four-component bilayer, DSPC/DOPC/POPC/CHOL. *Biophysical Journal*, 104(February), pp.853–862.

Gracià, R.S. et al., 2010. Effect of cholesterol on the rigidity of saturated and unsaturated membranes: fluctuation and electrodeformation analysis of giant vesicles. *Soft Matter*, 6, p.1472.

Heberle, F. a. et al., 2013. Bilayer thickness mismatch controls domain size in model membranes. *Journal of the American Chemical Society*, 135, pp.6853–6859.

Heberle, F. a. et al., 2010. Comparison of three ternary lipid bilayer mixtures: FRET and ESR reveal nanodomains. *Biophysical Journal*, 99(10), pp.3309–3318. Available at: http://dx.doi.org/10.1016/j.bpj.2010.09.064.

Kingsley, P. B., Feigenson, G.W., 1979. The Synthesis of a Perdueterated Phospholipid: 1,2-dimyristoyl-sn-glycero-3-phosphocholine-d72. *Chemistry and Physics of Lipids*, 24, pp.135–147.

Konyakhina, T.M. et al., 2011. Control of a nanoscopic-to-macroscopic transition: Modulated phases in four-component DSPC/DOPC/POPC/Chol giant unilamellar vesicles. *Biophysical Journal*, 101(2), pp.L8–L10. Available at: http://dx.doi.org/10.1016/j.bpj.2011.06.019.

Konyakhina, T.M. et al., 2013. Phase diagram of a 4-component lipid mixture: DSPC/DOPC/POPC/chol. *Biochimica et Biophysica Acta - Biomembranes*, 1828(9), pp.2204–2214. Available at: http://dx.doi.org/10.1016/j.bbamem.2013.05.020.

Kuzmin, P.I. et al., 2005. Line tension and interaction energies of membrane rafts calculated from lipid splay and tilt. *Biophysical journal*, 88(February), pp.1120–1133.

Nelson, F. et al., 2010. GUV Preparation and Imaging: Minimizing artifacts. *Biochimica et Biophysica Acta*, 1798(7), pp.1324–1332.

Petruzielo, R.S. et al., 2013. Phase behavior and domain size in sphingomyelin-containing lipid bilayers. *Biochimica et Biophysica Acta*, 1828, pp.1302–1313.

Reeves, J.P. & Dowben, R.M., 1969. Formation and properties of thin-walled phospholipid vesicles. *Journal of cellular physiology*, 73, pp.49–60.

Samsonov, a V, Mihalyov, I. & Cohen, F.S., 2001. Characterization of cholesterol-sphingomyelin domains and their dynamics in bilayer membranes. *Biophysical journal*, 81(3), pp.1486–1500. Available at: http://dx.doi.org/10.1016/S0006-3495(01)75803-1.

Semrau, S. et al., 2008. Accurate determination of elastic parameters for multicomponent membranes. *Physical Review Letters*, 100(February), pp.1–4.

Simons, K. & van Meer, G., 1988. Lipid sorting in epithelial cells. *Biochemistry*, 27(17), pp.6197–6202.

Simons, K. & Toomre, D., 2000. Lipid rafts and signal transduction. *Nature reviews. Molecular cell biology*, 1(October), pp.31–39.

Singer, S.J. & Nicolson, G.L., 1972. The fluid mosaic model of the structure of cell membranes. *Science (New York, N.Y.)*, 175(4023), pp.720–31. Available at: http://ressources.unisciel.fr/biocell/chap1/res/fluid mosaic model of cell membranes 1972-Singer.pdf\nhttp://www.ncbi.nlm.nih.gov/pubmed/4333397.

Tian, A. et al., 2007. Line tension at fluid membrane domain boundaries measured by micropipette aspiration. *Physical Review Letters*, 98(May), pp.18–21.